Chapter 5

Effect of different carbon and silicon sources for the preparation of ZrB_2-SiC composite powder: A comparative study

5. 1 Introduction

This research involved a unique approach incorporating graphite and carbon black as carbon sources and silicon and silica sources to prepare a ZrB_2-SiC composite under an argon atmosphere. The composite was synthesized using different carbon and silica sources, further phase analysis, and microstructural properties compared with each other. This chapter aimed to identify the most suitable sources of carbon and silica for producing the impurity-free ZrB_2-SiC composite. This study highlights the importance of carefully selecting the appropriate carbon and silica sources to produce ZrB_2-SiC composite powder with desirable microstructural properties. The formation of the composites in this study utilized a combination of starting reactants, including zirconia (ZrO_2), boron carbide (B_4C), Silica (SiO_2), silicon (Si), graphite (G), and carbon black (C). The detailed specification of the starting material is explained in Chapter 3.

The chemical reaction within the raw material can be expressed as follows.

$$ZrO_2(s) + 5/7B_4C(s) + Si(s) + C/G(s) \rightarrow ZrB_2(s) + SiC(s) + 3/7B_2O_3(l,g) + 5/7CO(g) \quad (5.1)$$

$$ZrO_2(s) + B_4C(s) + SiO_2(s) + C/G(s) \rightarrow ZrB_2(s) + SiC(s) + B_2O_3(s) + CO(s) \quad (5.2)$$

$$7ZrO_2(s) + 5B_4C(s) \rightarrow 7ZrB_2(s) + 3B_2O_3(g, l) + 5CO(g) \quad (5.3)$$

$$ZrO_2(s) + B_2O_3(g) + 5C(s) \rightarrow ZrB_2(s) + 5CO(g) \quad (5.4)$$

The group of the composition of ZrO_2, B_4C, Si/SiO_2, and graphite or carbon black was arranged according to Table 5.1. The powders were subjected to dry mixing via a high-energy mill (using a FRITSCH pulveristte 5) for 2 hours at 200 rpm with a zirconia ball (powder: ball-

1:10) used as the grinding agent. The resulting mixture was compacted under 12 Mpa pressure, with a diameter of 10 mm and thickness of 5 mm. The pellet was placed in a graphite crucible and inserted into a tube furnace. The furnace worked under moderate vacuum conditions of 10^{-2} torr and backfilled with Ar gas. All samples were processed stepwise, first at 900°C for 30 minutes and then at 1600°C for 180 minutes in a moderate vacuum with an argon supply, as shown in Fig. 5.1.

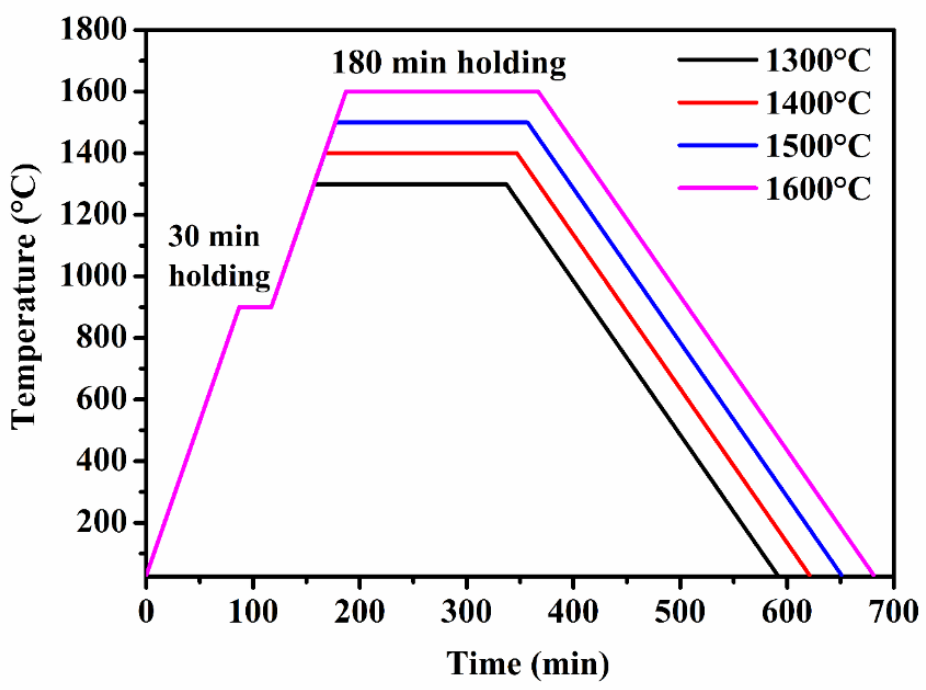

Fig. 5.1 The calcination process of ZrB_2-SiC ceramics

The expected wt % of the ZrB_2 and SiC composite powder was calculated by the first molar mass of the balanced reaction (1) and reaction (2). Subsequently, the total molar mass of ZrB_2 and SiC was determined by adding the molar masses of each product multiplied by their respective coefficients. Add the masses of the ZrB_2 and SiC products and express them as a percentage of the total mass of the products. Along with ZrB_2 and SiC, some 3/7 moles of B_2O_3(l) and 5/7 moles of CO(g) occur in reaction 5.1. similarly for the reaction 5.2, 1 mole of B_2O_3(l), and 1 mole of CO(g) takes place in the ZrB_2-SiC composite.

Table 5.1 The raw material composition used to prepare the composite includes ZrO_2, B_4C, Si/SiO_2, and graphite or carbon black.

Sample name	Mole content						Calculated (wt %)	
	ZrO_2	B_4C	Si	SiO_2	C	Graphite	ZrB_2	SiC
ZGSI	1	5/7	1	-	-	1	73.77	26.23
ZGSO	1	1	-	1	-	1	73.77	26.23
ZCSI	1	5/7	1	-	1	-	73.77	26.23
ZCSO	1	1	-	1	1	-	73.77	26.23

In comparison, the graphite and silica source required a high temperature (1600°C) for the complete conversion of oxides in the argon atmosphere. The schematic representation of in situ synthesized ZrB_2-SiC is illustrated in Fig. 5.2.

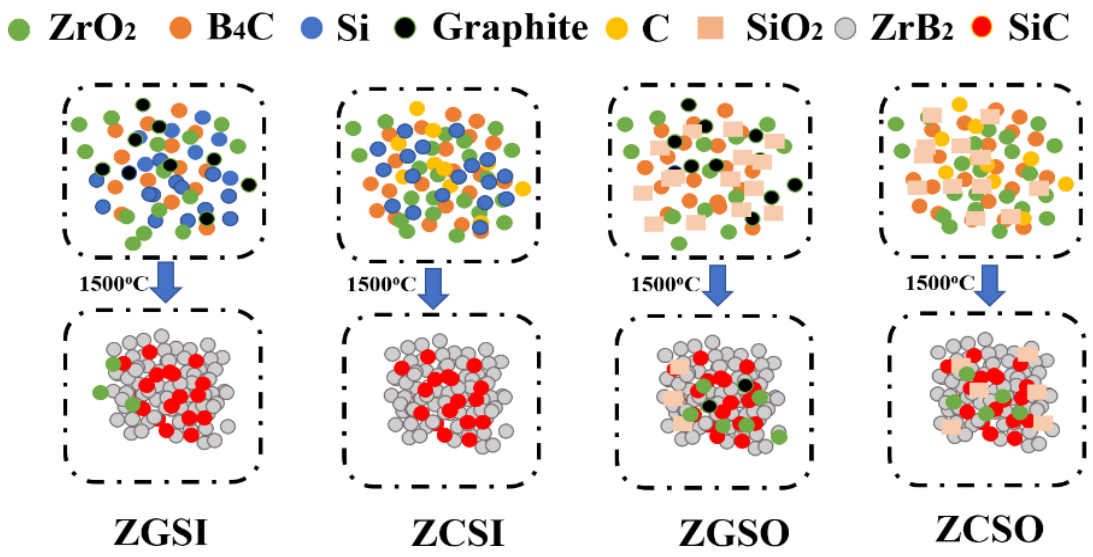

Fig. 5.2 The schematic representation of in situ synthesized ZrB_2-SiC composite.

5. 2 Result and discussion

5.2.1 Thermodynamic evolution of reactions

Their thermodynamic data can determine the feasibility of reactions at high temperatures. A reaction's standard Gibbs phase energy can be calculated based on its total free energy at a particular temperature, defining its feasibility. For instance, by utilizing FACTSage

thermochemical software, the thermodynamic calculation of a chemical reaction (5.1) was feasible under ambient pressure (P=1.013*105 Pa) at a temperature of 719.8°C [176]. Similarly, reaction (5.2) is possible at 1255.3°C, higher than reaction (5.1). The Gibbs energy of reaction (5.1) and reaction (5.2) is negative at 719.8 °C and 1255.3°C, respectively, and it increases due to the silica source used during synthesis shown in Fig.5.3.

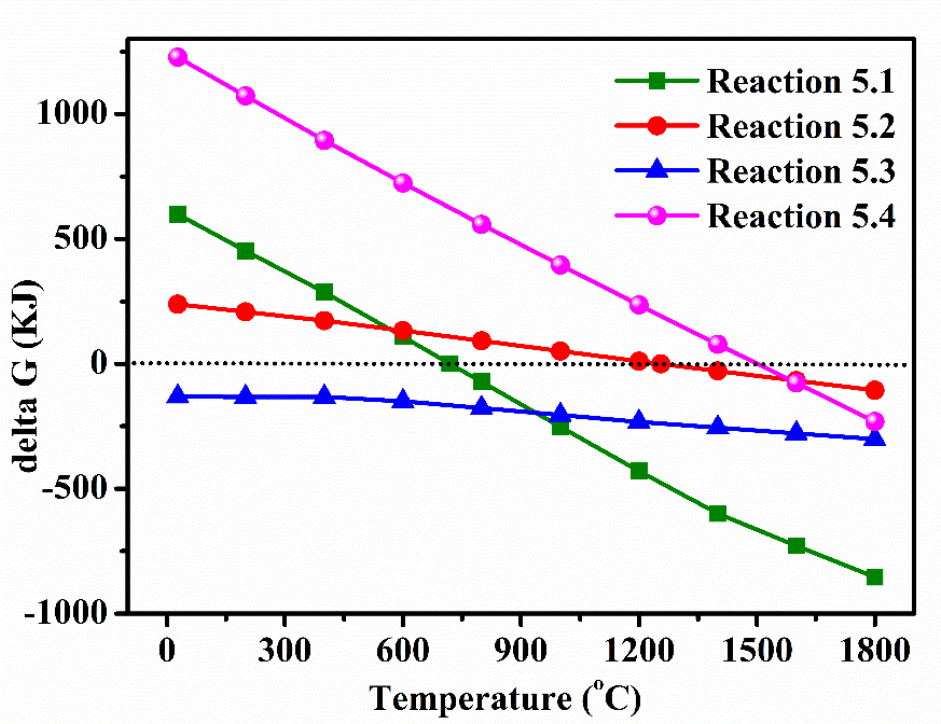

Fig. 5.3 Gibbs phase energy of reaction (5.1), (5.2), (5.3), and reaction (5.4) at various processing temperatures

5.2.2 Effect of calcination temperature on different carbon sources with silicon metal

Fig. 5.4 demonstrates the phase investigation of ZGSI at various temperatures. At 1300°C, a minor presence of ZrB_2 and SiC was studied, along with unreacted ZrO_2 and graphite. The formation of ZrB_2 occurs at 1300°C and higher temperatures [78]. At first, a portion of ZrO_2 undergoes a reaction with B_4C, forming an intermediate phase, B_2O_3, as stated in the chemical reaction (5.3). Afterward, this intermediate phase of B_2O_3 reacts with the

remaining ZrO_2, as depicted in a chemical reaction (4), ultimately yielding the production of ZrB_2.

By increasing the temperature to 1300-1600°C, a significant amount of ZrB_2 and SiC occurred, though minor ZrO_2 and graphite phases remained. As per Xie et al. [201], it remains uncertain whether the temperature range of 1500°C-1600 °C is adequate to transform graphite into SiC completely. However, the complete Si source reacts with graphite, and SiC occurs. At 1600°C, the whole reduction of graphite was confirmed through XRD analysis, with ZrB_2 and SiC weighing in at 68 % and 18%, respectively, as determined by the RRM. Along with ZrB_2, a minor ZrC phase is observed at 1600°C.

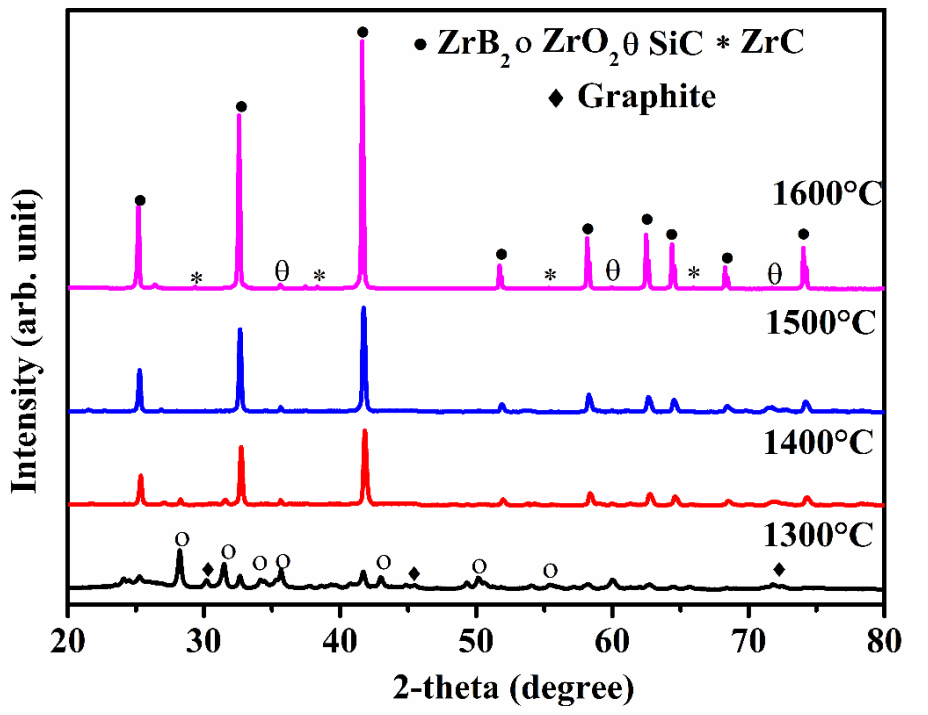

Fig. 5.4 XRD pattern of *ZGSI* samples at *1300-1600°C processing* temperature

The phase analysis of ZCSI at many temperatures ranging from 1300-1500°C is depicted in Fig. 5.5. The minor amount of ZrB_2 and SiC phase is confirmed with unreacted ZrO_2 and carbon observed at 1300°C. Continuing to raise the temperature until it reaches 1400°C, the SiC phase rises [180], but still, minor phases of ZrO_2 are present. Pure ZrB_2-SiC

composite is successfully obtained at 1500°C, i.e., increasing the calcination temperature positively affected the impurity-free composite. Also, carbon black was very helpful for reducing the synthesis reaction temperature and saving energy due to its high reactivity and amorphous nature. Carbon black has better reactivity as compared to graphite [50]. The better reactivity of the carbon is due to the layered and planar structure of graphite, where its primary conductivity takes place along its planes. Conversely, carbon black is characterized by its roughly spherical shape and sub-micron scale high surface area, which can aid in the reaction kinetics and lower the reaction temperature [202]. At temperatures up to 1500°C, the ZrB_2 and SiC composite powders had a pure phase, indicating that further temperature increases were unnecessary for the complete formation of the ZrB_2 and SiC composite powders.

The wt % of ZrB_2 and SiC is 72 % and 22 % at 1500°C, examined by the RRM, close to the theoretical value (73.77:26.23). The observed reduction in the ZrB_2 and SiC content may be attributed to the formation of boro-silicate phases or the complete conversion of the Si source into a vaporous state during the process [203]. The crystalline size of carbon-treated ZrB_2 and SiC for ZCSI are 107 nm to 55.3 nm, even though the graphite treated for ZGSI is 147.6 nm to 53.3 nm. The result demonstrated that the crystalline size of ZCSI is slightly lower than that of ZGSI. The smaller crystalline size can be described by the evidence that carbon has a smaller atomic size than graphite and silica. The Scherer equation determines the crystalline size.

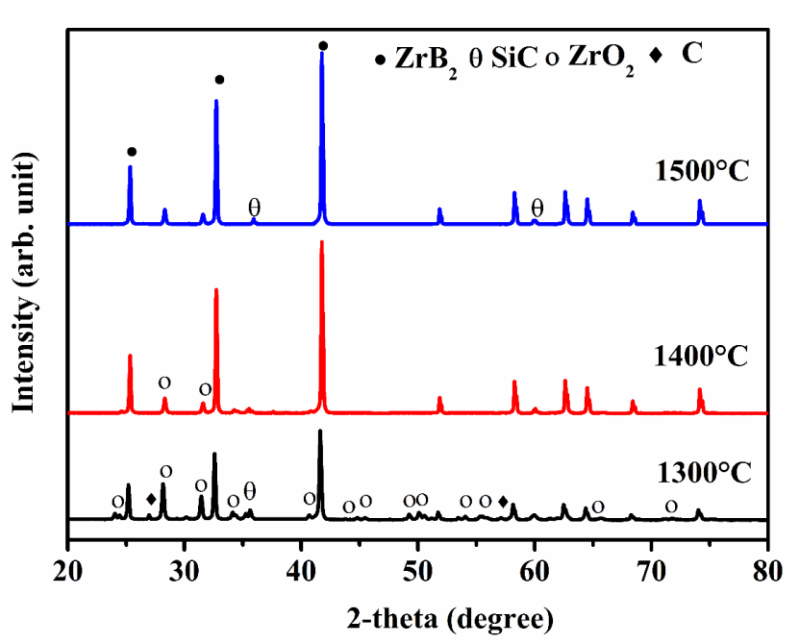

Fig. 5.5 XRD pattern of *ZCSI* samples at *1300-1500°C processing* temperature

5.2.3 Effect of calcination temperature on different carbon sources with silica

The phase analysis of calcined ZGSO and ZCSO at various temperatures is depicted in Figs. 5.6 and 5.7, respectively. At 1300°C, the XRD pattern confirms the presence of a minor amount of ZrB_2 and SiC phases alongside unreacted ZrO_2 and graphite phases. As the temperature increases from 1300°C to 1500°C, the XRD pattern shows a significant increase in ZrB_2 and SiC powders. However, minor phases of ZrO_2 and carbon source are still observed in both composites. When there is a presence of an oxide impurity called ZrO_2 at lower temperatures, it encourages the grains to become more significant. However, oxide impurities can hinder the densification process, forming pores within the grains. The pores become trapped as the temperature increases continuously, reaching up to 1600°C. A small amount of ZrO_2 phase has been detected in the composite materials ZGSO and ZCSO. For instance, Zhang et al. [204] found that the complete conversion of graphite into SiC occurred at 1650-1800°C. However, the conversion rate was relatively low at this temperature range, requiring longer

reaction times. The reaction (5.5) was determined to form SiC when silica and carbon/graphite were present.

$$SiO_2\ (s) + 3C\ (s) \rightarrow SiC\ (s) + 2CO\ (g) \qquad (5.5)$$

As the temperature increases below the melting point of SiO_2, the reaction described in reaction (6) becomes more predominant. Thus, this leads to a reduced release of SiO, and a more significant SiC formation occurs between 1450°C and 1475°C [205], while Baumann observed that the process begins at 1500°C [206]. The wt % of ZrB_2 and SiC is 70 % and 15 % for ZGSO and 71 % and 16 % for ZCSO, analyzed by the RRM. The crystalline of ZrB_2 and SiC for ZGSO is 237.6 nm to 83.3 nm, and for ZCSO is 161 nm to 75 nm.

It is essential to acknowledge that the final product's actual amount is typically lower than the considered value, which may be due to the formation of the B_2O_3 product during the one-step carbothermal reduction process. The transitional B_2O_3 is known to have a lower melting point (450°C) and high vapor pressure [86,207], which results in its rapid vaporization at high temperatures.

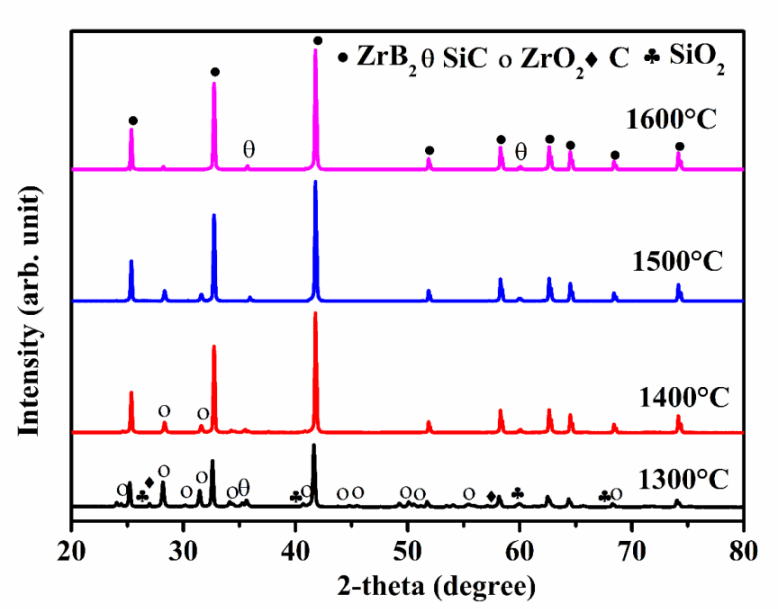

Fig. 5.6 XRD pattern of *ZCSO* samples at *1300-1600°C processing* temperature

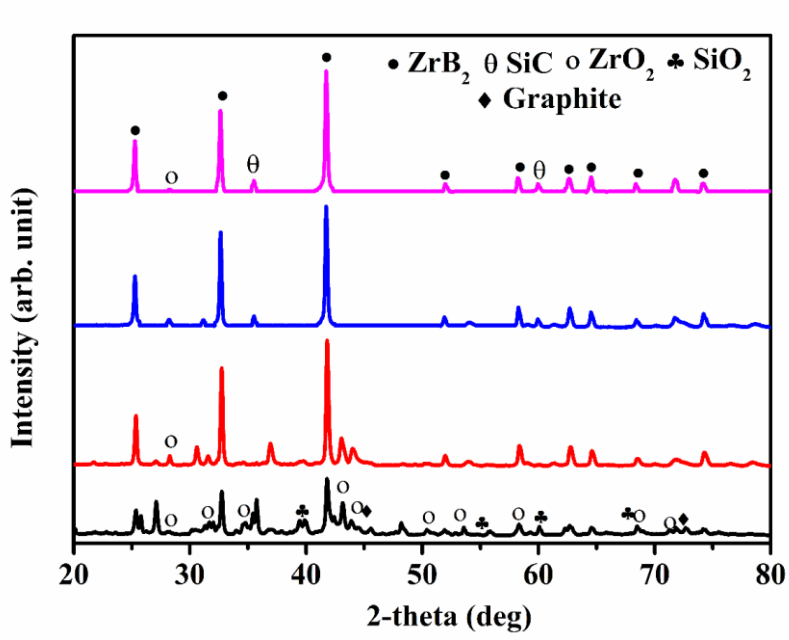

Fig. 5.7 XRD pattern of *ZGSO* samples at *1300-1600°C processing* temperature

5.2.4 Microstructure with the different carbon and silicon source

Fig. 5.8 (a) and Fig. 5.8 (b) show the microstructure and morphology of the *ZGSI and ZCSI* samples, respectively. In Fig. 5.8(a), two distinct low-sub-angular spherical particles (Φ 0.2-1 μm) are observed, along with multiple sub-rounded tiny particles distributed throughout the composite. Similarly, Fig. 5.8 (b) depicts two structures in the ZCSI sample: sub-angular micron-sized granules and small particles. EDS analysis was used to verify the elemental compositions of the ZrB_2-SiC composite. The EDS analysis confirmed the presence of Zr, B, Si, and C elements in both composites. The SEM image shows that the tiny particles were distributed in the ZrB_2 composite, which had uniform grain sizes and morphology. This uniform distribution of small particles prevented the growth of ZrB_2 phase grains and promoted densification [95]. In Fig. 5.8 (b) for ZCSI, the particle dimensions were decreased compared to sample ZGSI in Fig. 5.8 (a), resulting in a uniform microstructure attributed to the grain growth-inhibiting effect of SiC. Literature suggests optimizing carbon content leads to total

oxide conversion into ZrB_2-SiC, resulting in a homogeneous and small-scale morphology [197].

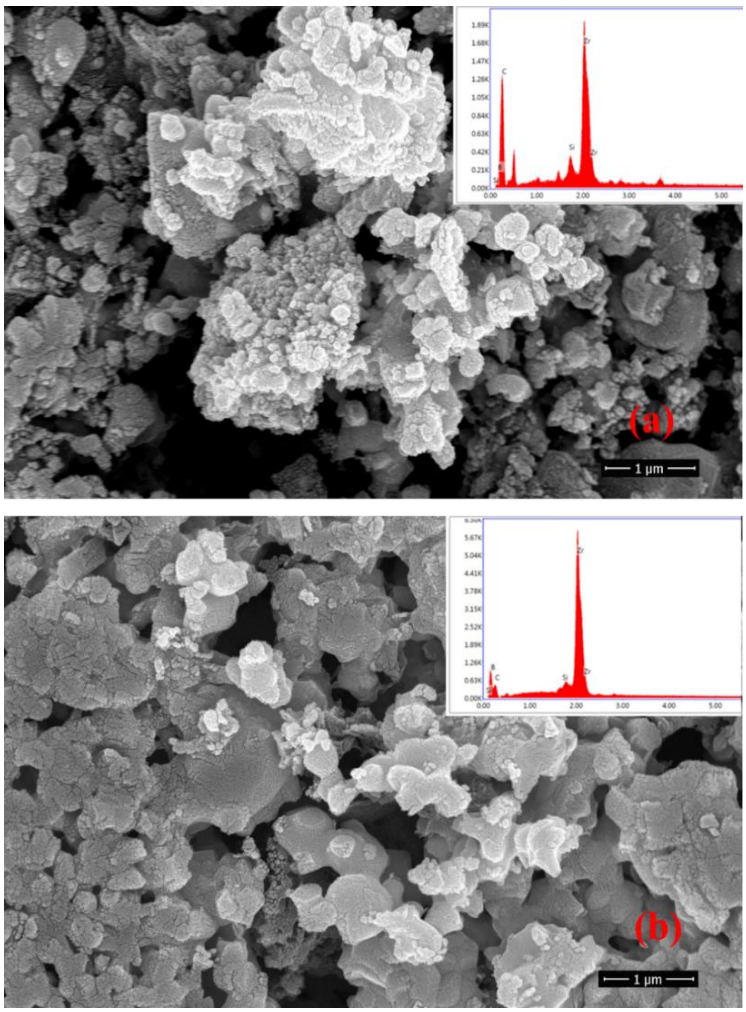

Fig. 5.8 FE-SEM of the (a) ZGSI (b) ZCSI samples at *1500°C*

Fig. 5.9 (a) and Fig. 5.9 (b) depict the particle microstructure and micrographs of ZGSO and ZCSO, respectively, at a temperature of 1500°C. Fig. 5.9 (a) illustrates the morphology of the ZGSO sample; it consists of large irregular cluster particles along with a few small particles. In contrast, the SEM image of *ZCSO* in Fig. 5.9 (b) consists of small irregular clusters after calcination. The particle size of ZGSO was larger than sample ZCSO, which may be due to unreacted silica and graphite particles in the final composition confirmed in the XRD analysis. The presence of oxide impurities contributes to decreased densification during the calcination process.

The EDS analysis confirmed that the elemental composition of ZCSO and ZGSO was composed of Zr, B, C, Si, and O. The O presented in the EDS analysis may be due to the presence of oxide in the ZrB_2-SiC composite. These observations suggest that a proper amount of SiC content is crucial for achieving optimal microstructure in ZrB_2-SiC composites at high temperatures.

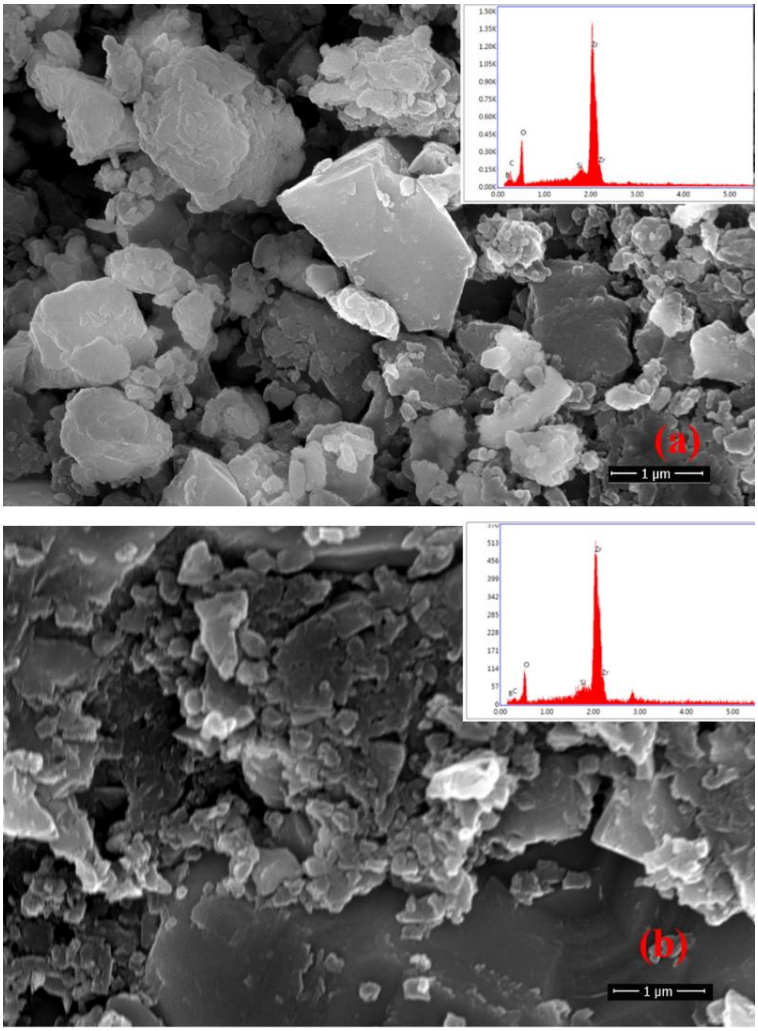

Fig. 5.9 FE-SEM of the (a) ZGSO (b) ZCSO samples at *1500°C*

Based on the above observation, it can be concluded that the silicon source with carbon (*ZCSI samples*) produces an impurity-free sample even at a lower temperature. Thus, among all compositions, the focus was shifted to analyzing the ZCSI composite using transmission electron microscopy (TEM), as revealed in Fig. 5.10 (a)- Fig (b). Fig 5.10 (a) illustrates the

average particle size ranging from 200 nm to 500 nm for the ZCSI composite. Fig. 5.10 (b) displays the selected electron area diffraction (SEAD) pattern at the junction of the ZCSI composite, which includes the (001), (012), and (021) planes of ZrB_2 and (002) crystal plane of SiC. The measured d-spacing values derived from the crystal planes identified in the SAED pattern exhibit a remarkable consistency with the corresponding values reported in the X-ray Diffraction (XRD) JCPDS card for ZrB_2 and SiC. This unity supports the accurate identification of crystal planes within the SAED pattern, ensuring that the observed lattice spacings match the established values for ZrB_2 and SiC. TEM was used to confirm that the ZrB_2 and SiC powders were successfully synthesized. The TEM results showed the presence of the crystal structure of ZrB_2 and SiC. TEM results ensure the successful synthesis of ZrB_2 and SiC powders, essential components of the ZCSI composite.

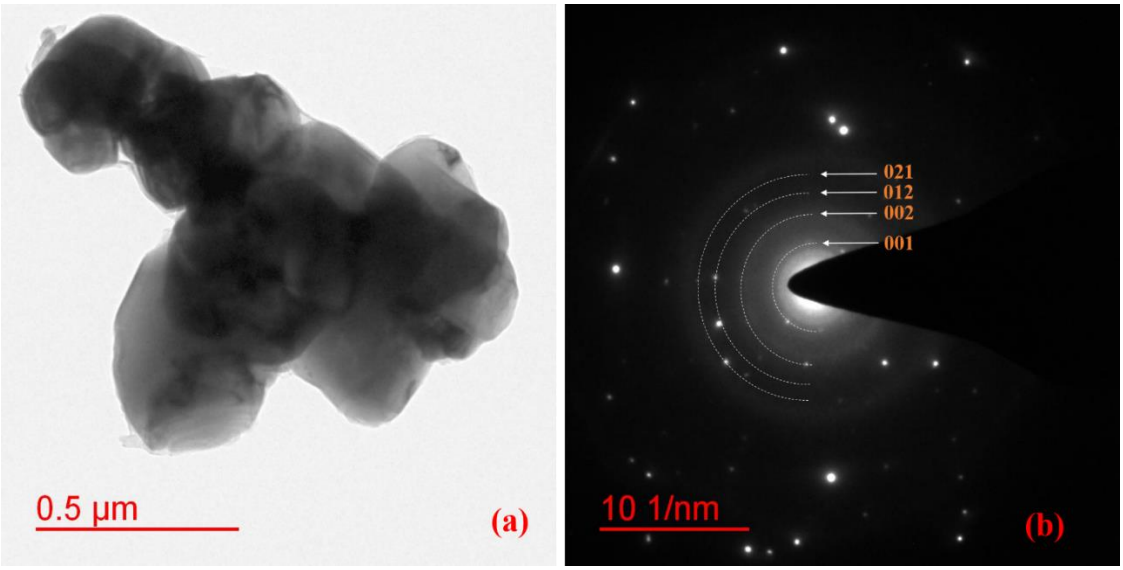

Fig. 5.10 (a). TEM image (b) SEAD pattern of the impurity-free ZCSI samples at 1500 °C

5. 3 Conclusion/ Summary of the chapter

The ZrB_2-SiC composite was synthesized by the one-step reduction method using Si/SiO_2, ZrO_2 B_4C, and different carbon sources. The result was as follows:

1. The ZCS1 and ZCSO have a lower synthesis temperature than ZGS1 and ZGSO. It is attributed to high surface area particles and the amorphous nature, consequently leading to better reactivity.
2. The ZGS1 samples were heated to 1500°C and contained impurities of ZrO_2 and graphite. In contrast, the ZSC1 composite obtained pure ZrB_2 and SiC at the same temperature.
3. The silica source with carbon or graphite (ZGSO/ ZCSO) at 1500°C had a high amount of oxide impurity due to a slow reaction rate. Increasing the temperature up to 1600°C sharply increases the reaction rate. Therefore, increasing the temperature can improve the efficiency of the reaction and reduce the oxide impurity levels of the ZGSO/ ZCSO composite.
4. The crystalline size ZCS1 is lower than the ZGS1, ZGSO, and ZCSO. It decreases with Si and C content compared to silica and graphite sources due to reduced oxide impurity in the composite. The interaction between silicon and carbon in the composite material is also stronger, contributing to the smaller crystalline size.
5. The SEM result revealed that the microstructure of ZCS1 and ZGS1 produced particles of nearly spherical angular shape. Silica with carbon (ZCSO) includes small irregular clusters and columnar particles, whereas silica with graphite (ZGSO) results in large irregular shapes with tiny cluster particles containing oxide impurities.